

具有可逆热致变色有机-无机杂化铜化合物的合成及表征

李明丽 张秀秀 饶文俊 魏振宏* 王玲玉 蔡 琥*

(南昌大学化学学院, 南昌 330031)

摘要: 在浓盐酸水溶液中, 碘化 *N,N*-二甲基-1,5-二氮杂环[3.2.1]辛烷([3.2.1-Me₂dabco]I₂)和碘化 1-氨基-1,4-二氮杂环[2.2.2]辛烷([2.2.2-NH₂dabco]I)与氯化铜反应得到 2 种有机-无机杂化铜化合物[3.2.1-Me₂dabco][CuCl₄] (**1**)和[2.2.2-NH₂dabco][CuCl₄] (**2**)。X 射线单晶结构衍射证实化合物 **1** 和 **2** 中的无机阴离子是[CuCl₄]²⁻四面体。化合物 **1** 和 **2** 表现出可逆的热致变色现象, 随着温度升高, 它们的颜色从黄色变为红色, 这应该是由[CuCl₄]²⁻四面体的变形引起的。

关键词: 1,4-二氮杂二环[2.2.2]辛烷; 氯化铜; 热致变色; 有机无机杂化; 晶体结构

中图分类号: O723; O799 文献标识码: A 文章编号: 1001-4861(2020)06-1137-06

DOI: 10.11862/CJIC.2020.118

Synthesis and Characterization of Two Organic-Inorganic Hybrid Copper(II) Compounds with the Reversible Thermochromism

LI Ming-Li ZHANG Xiu-Xiu RAO Wen-Jun WEI Zhen-Hong* WANG Ling-Yu CAI Hu*

(College of Chemistry, Nanchang University, Nanchang 330031, China)

Abstract: Reactions of *N,N*-dimethyl-1,5-diazabicyclo[3.2.1]octane iodide ([3.2.1-Me₂dabco]I₂) and 1-amino-1,4-diazabicyclo[2.2.2]octane iodide ([2.2.2-NH₂dabco]I) with anhydrous copper chloride in concentrated HCl aqueous solution afforded two organicinorganic hybrid compounds [3.2.1-Me₂dabco][CuCl₄] (**1**) and [2.2.2-NH₂dabco][CuCl₄] (**2**), respectively. The single-crystal X-ray diffraction revealed that the inorganic component in compounds **1** and **2** was a distorted tetrahedral geometry [CuCl₄]²⁻. Compounds **1** and **2** showed an intriguing reversible thermochromism with color change from yellow to red which may be derived from the deformation of [CuCl₄]²⁻ tetrahedron. CCDC: 1983284, **1**; 1983282, **2**.

Keywords: 1,4-Diazabicyclo[2.2.2]octane; copper chloride; thermochromism; organic-inorganic hybrid; crystal structure

Thermochromism, the phenomenon of reversible change of color with change of temperature has been studied for decades due to their potential applications in the smart windows, temperature sensors, visual thermometers and solar control glazing^[1-6]. In past years, immense efforts have been devoted to preparation an extensive range of novel thermochromic material classes, including the conventional inorganic solids like vanadium dioxide^[7], hydrogels^[8], polymers^[9-10], syn-

thetic dyes^[11], organic crystals^[12], coordination complexes^[13-14], and organic-inorganic hybrid compounds^[15-16].

Among these different kinds of thermochromic materials, organic-inorganic hybrid compounds have received extraordinary research attention because of their structural advantages^[17-18]. In these hybrids, the presences of inorganic components supply excellent electronic properties and mechanical and thermal stability, and the organic components ensure structural

收稿日期: 2020-02-19。收修改稿日期: 2020-04-01。

国家自然科学基金(No.21571094, 21661021, 21865015)资助项目。

*通信联系人。E-mail: weizh@ncu.edu.cn

flexibility and synthetic versatility^[19-20]. Detailed studies on the reversible thermochromic properties of organic-inorganic hybrid compounds revealed the origins were most attributed to the change of coordination geometry, bond breakage/formation, dynamic structural change, charge transfer, and mode of coordinating ligand^[21].

On the other hand, temperature-induced reversible phase transitions have been common observed in the copper(II) organic-inorganic complexes^[22-25], which were mostly caused by the change in coordination number and coordination geometry^[26-28]. This is because that the color is limited by the energy of *d-d* electronic transitions of central Cu²⁺ ion in organic-inorganic Cu(II) halide system, where the color change generally in the range from green to red, including green to yellow, yellow to brown and yellow to red^[29-31]. For examples, the known organic-inorganic hybrid compounds [(C₂H₅)₂NH₂][CuCl₄]^[32], [(2-aminobenzothiazolium)₂][CuCl₄]^[33] and [DMe-DABCO][CuCl₄] (*N,N'*-dimethyl-1,4-diazoniabicyclo [2.2.2]-octonium)^[34] have been reported to exhibit reversible thermochromism.

In this paper, two spherical organic molecules 1-amino-1,4-diazabicyclo [2.2.2]octane-1,4-diium iodide ([2.2.2-NH₂dabco]I) and *N,N*-dimethyl-1,5-diazabicyclo [3.2.1]octane iodide ([3.2.1-Me₂dabco]I₂) were synthesized and chosen to react with CuCl₂, and finally led to the formation of tetrahedrally coordinated organic-inorganic hybrid compounds [3.2.1-Me₂dabco][CuCl₄] (**1**) and [2.2.2-NH₂dabco][CuCl₄] (**2**). Herein, we report the crystal structure and reversible thermochromism of **1** and **2**.

1 Experimental

1.1 Instruments and materials

The starting materials anhydrous CuCl₂, 1,4-diazabicyclo [2.2.2]octane, 1,5-diazabicyclo [3.2.1]octane and the concentrated hydrochloric acid are commercially available and used without further purification. 1-Amino-1,4-diazabicyclo [2.2.2]octane-1,4-diium iodide ([2.2.2-NH₂dabco]I)^[35] and *N,N*-dimethyl-1,5-diazabicyclo [3.2.1]octane iodide ([3.2.1-Me₂dabco]I₂)^[36] were synthesized according the reported literatures. Powder X-ray diffraction data of **1** and **2**

were recorded on an X-ray powder diffractometer (Beijing Persee Instrument Co., Ltd. XD-3) with Cu *K*α radiation (λ=0.154 06 nm) operating at 40 kV/15 mA with a *K*β foil filter at a speed of 2°·min⁻¹ in a range of 5.00° ≤ 2θ ≤ 55.00°. Elemental analysis of C, H and N were conducted on a Vario EL III elemental analyzer.

1.2 Synthesis

1.2.1 *N,N*-dimethyl-1,5-diazabicyclo[3.2.1]octane iodide ([3.2.1-Me₂dabco]I₂)

To a 40 mL methanol solution of 1,5-diazabicyclo [3.2.1]octane (4 g, 36 mmol) was dropwise added CH₃I (76 mmol, 10.5 mL). After addition, the reaction was refluxing for 3.5 hours, and led to the formation of gray precipitate, which was isolated by filtration and washed with hot ethyl acetate, dried *in vacuo*. Yield: 1.6 g, 95%. ¹H NMR (400 MHz, D₂O): δ 5.35 (s, 2H), 4.45 (d, *J*=6.7 Hz, 2H), 4.24 (dd, *J*=16.1, 11.0 Hz, 2H), 4.10~3.85 (m, 4H), 3.55 (s, 6H), 2.79 (m, *J*=25.6, 19.3, 12.8, 6.5 Hz, 1H), 2.55 (d, *J*=16.4 Hz, 1H).

1.2.2 1-Amino-1,4-diazabicyclo[2.2.2]octane iodide ([2.2.2-NH₂dabco]I)

To an aqueous solution (20 mL) of 2.2.2-dabco (16.80 g, 150.0 mmol) was dropwise added an aqueous solution (10 mL) of H₂NOSO₃H (5.65 g, 50.0 mmol) at the temperature of 90 °C under the N₂ atmosphere. After the mixture was cooled to room temperature, K₂CO₃ (6.90 g, 50.0 mmol) was added. The resulting mixture was stirring for 10 minutes, then the solvent was removed by vacuum-rotary evaporation, and the crude residue was washed by tetrahydrofuran (THF) for 3 times. The residue was collected and dissolved in 30 mL EtOH, and K₂CO₃ was removed by filtration. The filtrate was acidized by the addition of 7.0 mL hydriodic acid (11.0 g, 57% (*w/w*)). The reaction mixture was allowed to be stirring at -30 °C for 1 hour to give pale-yellow precipitates, which were filtered and washed with EtOH to afford the desired product as a white solid. Yield: 6.5 g, 34%. ¹H NMR (400 MHz, D₂O): δ 3.87~3.78 (m, 6H), 3.67~3.58 (m, 6H); ¹³C NMR (100 MHz, D₂O): δ 56.4, 44.7.

1.2.3 [3.2.1-Me₂dabco][CuCl₄] (**1**)

To an aqueous solution of [3.2.1-Me₂dabco]I₂

(1.98 g, 5 mmol) was added Ag_2CO_3 (0.7 g, 2.54 mmol) solid. The mixture was kept stirring for 2 hours and filtered. The filtrate was acidized with 8 mL hydrochloric acid (36%(w/w)), and anhydrous CuCl_2 (0.67 g, 5 mmol) was added. The yellow block crystal was obtained by volatilizing the solution at 40 °C for three days. Yield: 2.69 g, 80%. Anal. Calcd. for $\text{C}_8\text{H}_{16}\text{N}_2\text{CuCl}_4$ (%): C, 27.81; H, 4.67; N, 8.11. Found(%): C, 28.12; H, 4.45; N, 8.28.

1.2.4 [2.2.2- NH_2dabco][CuCl_4] (**2**)

To a concentrated HCl aqueous solution (10 mL, 36%) was added [2.2.2- NH_2dabco]**I** (2.55 g, 10.0 mmol) and anhydrous CuCl_2 (1.35 g, 10.0 mmol). Evaporation of the solution gave the yellow rod-like crystals at room temperature in three days. The crystals were filtered and washed with ethanol and dried *in vacuo*. Yield: 2.51 g, 75%. Anal. Calcd. for $\text{C}_6\text{H}_{15}\text{N}_3\text{CuCl}_4$ (%): C, 21.54; H, 4.52; N, 12.56. Found (%): C, 21.25; H,

4.32; N, 13.02.

1.3 X-ray crystallography

Diffraction data of the single crystals with dimensions of 0.14 mm×0.18 mm×0.15 mm for **1** and 0.26 mm×0.10 mm×0.12 mm for **2** were collected on a Bruker SMART CCD area detector diffractometer with graphite monochromated Mo $K\alpha$ radiation ($\lambda = 0.071\ 073\ \text{nm}$). The crystal structures were solved by direct methods using SHELXL^[37]. Non-hydrogen atoms were first refined isotropically followed by anisotropic refinement by full matrix least-squares calculations based on F^2 . Hydrogen atoms on carbon and nitrogen atoms were placed in idealized positions and treated as riding atoms. Crystal data and structure refinement results of compounds **1** and **2** were summarized in Table 1.

CCDC: 1983284, **1**; 1983282, **2**.

Table 1 Crystallographic data for compounds **1** and **2**

Compound	1	2
Formula	$\text{C}_8\text{H}_{16}\text{N}_2\text{CuCl}_4$	$\text{C}_6\text{H}_{15}\text{N}_3\text{CuCl}_4$
Formula weight	345.58	334.56
Crystal system	Monoclinic	Monoclinic
Space group	$P2_1$	$P2_1/c$
a / nm	0.730 21(7)	0.847 21(10)
b / nm	1.399 02(14)	1.112 84(12)
c / nm	0.755 73(7)	1.337 36(16)
$\beta / (^\circ)$	115.626 0(10)	92.399(2)
V / nm^3	0.696 10(12)	1.259 8(3)
Z	2	4
$D_c / (\text{g} \cdot \text{cm}^{-3})$	1.649	1.764
$F(000)$	350	676
θ_{max}	26.66	27.51
$\mu / \text{mm}^{-1} (\text{Mo } K\alpha)$	2.308	2.549
Total reflections	4 262	7 394
Unique reflections	2 991	2 860
No. of variables	136	136
R_1, wR_2 (observed data)	0.029 0, 0.060 9	0.028 4, 0.069 5
R_1, wR_2 (all data)	0.034 3, 0.063 0	0.032 9, 0.072 1
GOF	0.958	1.105

2 Results and discussion

2.1 Synthesis and characterization

The two caged organic amines [3.2.1- Me_2dabco]**I**₂

and [2.2.2- NH_2dabco]**I** were synthesized according to the literatures with little modifications^[35-36], and their corresponding organic-inorganic hybrid copper (II) compounds [3.2.1- Me_2dabco][CuCl_4] (**1**) and [2.2.2-

$\text{NH}_2\text{dabco}][\text{CuCl}_4]$ (**2**) were obtained by reactions with CuCl_2 on the basis of molar ratio of 1 : 1 in concentrated hydrochloric acid. Their phase purities were verified using the elemental analysis (EA) and powder X-ray diffraction (PXRD) patterns. As shown in Fig.1, the experimental PXRD curves of **1** and **2** were matched very well with the simulated ones in terms of the single-crystal X-ray data.

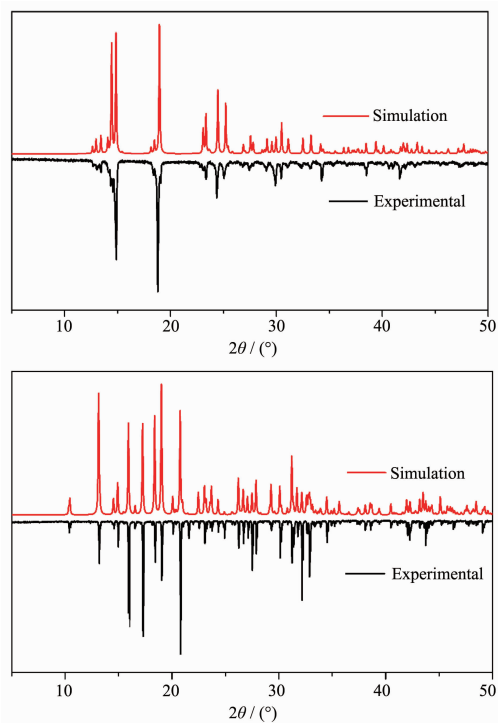


Fig.1 PXRD patterns of compounds **1** (above) and **2** (below) with the simulated one in red and the experimental one in black

2.2 Crystal structure analysis

Compound **1** crystallizes in the monoclinic

system with $P2_1$ space group, and the asymmetric unit contains one independent $[\text{CuCl}_4]^{2-}$ anion and one $[\text{3.2.1-Me}_2\text{dabco}]^{2+}$ cation, as shown in Fig.2. In the $[\text{3.2.1-Me}_2\text{dabco}]^{2+}$ cation, the two positive charges are supplied by two quaternary nitrogen atoms. In the $[\text{CuCl}_4]^{2-}$ anion, the central Cu^{2+} ion adopts a tetrahedral geometry coordinated by four Cl^- ions. As shown in Table 2, compound **1** has four independent Cu-Cl bond distances ranging from 0.221 62(17) to 0.223 05(11) nm and six independent bond angles $\angle \text{Cl-Cu-Cl}$ varying from $100.28(4)^\circ$ to $128.28(4)^\circ$, indicating a slightly distortion of the $[\text{CuCl}_4]^{2-}$ tetrahedron in **1**.

Compound **2** crystallizes in the monoclinic system with a space group of $P2_1/c$ and the asymmetric unit contains one protonated $[\text{2.2.2-NH}_2\text{dabco}]^{2+}$ cation and one $[\text{CuCl}_4]^{2-}$ anion, as shown in Fig.3. In the $[\text{2.2.2-NH}_2\text{dabco}]^{2+}$ cation, only the tertiary amine nitrogen atom N(3) is protonated, and the primary amine nitrogen N(1) can't be protonated. The two positive charges in $[\text{2.2.2-NH}_2\text{dabco}]^{2+}$ cation are expressed by one quaternary nitrogen atom N (2) and one tertiary

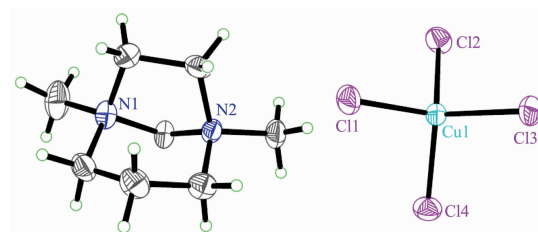


Fig.2 Crystal structures of **1** in the asymmetric unit with the displacement ellipsoids drawn at the 50% probability level

Table 2 Selected bonds (nm) and angles ($^\circ$) for **1** and **2**

1					
Cu1-Cl1	0.223 45(9)	Cu1-Cl3	0.223 37(9)		
Cu1-Cl2	0.223 26(9)	Cu1-Cl4	0.224 84(9)		
Cl2-Cu1-Cl3	100.28(4)	Cl3-Cu1-Cl1	128.23(4)	Cl3-Cu1-Cl4	102.01(4)
Cl2-Cu1-Cl1	101.43(4)	Cl2-Cu1-Cl4	128.28(4)	Cl1-Cu1-Cl4	100.18(4)
2					
Cu1-Cl1	0.223 28(6)	Cu1-Cl3	0.225 22(6)		
Cu1-Cl2	0.226 13(6)	Cu1-Cl4	0.226 19(6)		
Cl2-Cu1-Cl3	130.39(2)	Cl3-Cu1-Cl1	101.29(2)	Cl3-Cu1-Cl4	97.79(2)
Cl2-Cu1-Cl1	100.16(2)	Cl2-Cu1-Cl4	101.11(2)	Cl1-Cu1-Cl4	130.63(3)

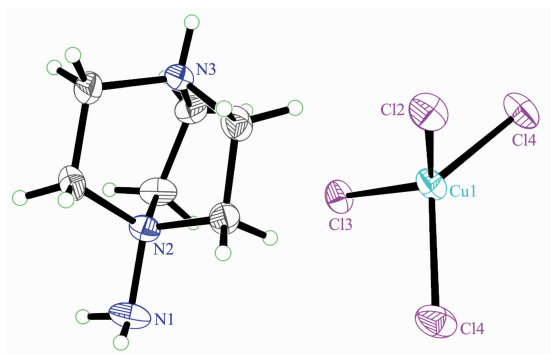


Fig.3 Crystal structures of **2** in the asymmetric unit with the displacement ellipsoids drawn at the 50% probability level

protonated N(3) atom. Similar to compound **1**, the metal center Cu^{2+} ion in the $[\text{CuCl}_4]^{2-}$ anion is also tetrahedrally coordinated by four Cl^- ions. As shown in Table 2, the Cu-Cl bond lengths in compound **2** varied from 0.223 28(6) to 0.226 19(6) nm, and the bond angles $\angle \text{Cl-Cu-Cl}$ range from $97.79(2)^\circ$ to $130.63(3)^\circ$, which are larger than the corresponding ones in compound **1**, revealing the $[\text{CuCl}_4]^{2-}$ tetrahedron in compound **2** is slightly distorted than that in compound **1**.

In compound **1**, there is no hydrogen bond between the cation and the $[\text{CuCl}_4]^{2-}$ anion, and the $\angle \text{Cl-Cu-Cl}$ angles are less than 130° . While, in compound **2** the cations and anions are connected by three kinds of $\text{N-H}\cdots\text{Cl}$ hydrogen bonds extending indefinitely in the two-dimensional (2D) ac plane as shown in the Fig.4. Due to the existing of $\text{N-H}\cdots\text{Cl}$ hydrogen bonding (Table 3), the maximum $\angle \text{Cl-Cu-Cl}$ angle of $130.63(3)^\circ$ in compound **2** is slightly larger than 130° .

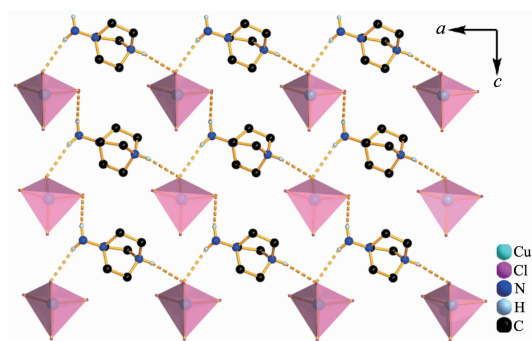


Fig.4 Hydrogen bonds connected the cations and anions in compound **2**

Table 3 Hydrogen bonds in compound **2**

D-H \cdots A	$d(\text{D-H}) / \text{nm}$	$d(\text{H}\cdots\text{A}) / \text{nm}$	$d(\text{D}\cdots\text{A}) / \text{nm}$	$\angle \text{DHA} / (^\circ)$
N(1) ⁱ -H(1c) \cdots Cl(4)	0.095(3)	0.267(3)	0.355 6(2)	155(3)
N(1) ⁱⁱ -H(1e) \cdots Cl(2)	0.089(3)	0.256(3)	0.339 1(2)	156(3)
N(3) ⁱⁱⁱ -H(3c) \cdots Cl(2)	0.091	0.258	0.329 80(17)	136

Symmetry codes: ⁱ $2-x, -1/2+y, 1/2-z$; ⁱⁱ $2-x, 1-y, 1-z$; ⁱⁱⁱ $1-x, 1-y, 1-z$

2.3 Thermochromism

Interestingly, the crystals **1** and **2** both exhibited yellow color at room temperature. When the temperature exceeds 60°C , the yellow crystals **1** and **2** gradually changed from yellow into red. Conversely, the red crystals were reversed to yellow completely upon cooling to room temperature in just few minutes, exhibiting reversible thermochromism, in Fig.4. To our best knowledge, thermochromism is commonly seen in other tetrahedrally coordinated Cu(II) halides, where the Cu^{2+} ion has the $3d^9$ electronic configuration, and the d -level is not completely filled^[38-39]. Consequently, there are $d-d$ electronic transitions within the $3d^9$ electronic configuration. Since the position of the absorption maximum for the $d-d$ transition is

correlated with the coordination geometry of central Cu^{2+} ion, the deformation of Cu(II) halide polyhedron in the structure will cause the shift of electronic absorption bands, which induces the color change of organic-inorganic Cu(II) halides. Therefore, in **1** and **2**,

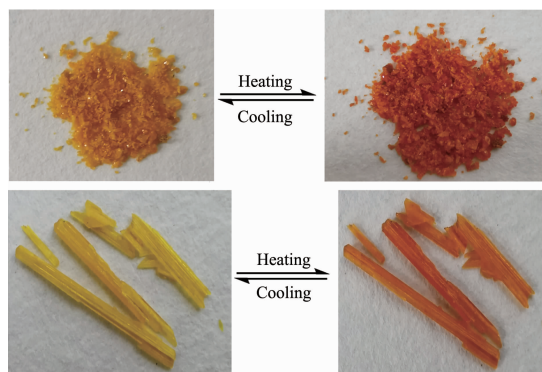


Fig.5 Reversible thermochromism in **1** (top) and **2** (bottom)

the remarkable deformation of $[\text{CuCl}_4]^{2-}$ tetrahedron is responsible for the yellow-to-red color change.

3 Conclusions

In summary, reactions of *N,N*-dimethyl-1,5-diazabicyclo [3.2.1]octane iodide ($[\text{3.2.1-Me}_2\text{dabco}]\text{I}_2$) and 1-amino-1,4-diazabicyclo [2.2.2]octane iodide ($[\text{2.2.2-NH}_2\text{dabco}]\text{I}$) with anhydrous CuCl_2 led to two organic-inorganic hybrid compounds $[\text{3.2.1-Me}_2\text{dabco}][\text{CuCl}_4]$ (**1**) and $[\text{2.2.2-NH}_2\text{dabco}][\text{CuCl}_4]$ (**2**) which were characterized by element analysis, single X-ray diffraction and powder X-ray diffraction. Crystals **1** and **2** showed reversible thermochromism, and the deformation of $[\text{CuCl}_4]^{2-}$ tetrahedron was responsible for the yellow to red color change.

Acknowledgement: We thank the National Natural Science Foundation of China (Grants No.21571094, 21661021, 21865015) for financial support.

References:

- [1] Ma X H. *Chin. J. Chem.*, **2019**,**37**:1287-1288
- [2] Pitchaimani J, Karthikeyan S, Lakshminarasimhan N, et al. *ACS Omega*, **2019**,**4**:13756-13761
- [3] Sun B, Liu X F, Li X Y, et al. *Angew. Chem. Int. Ed.*, **2020**, **59**:203-208
- [4] Yu T L, Guo Y M, Wu G X, et al. *Coord. Chem. Rev.*, **2019**, **397**:91-111
- [5] Li G P, Hao P F, Shen J J, et al. *Inorg. Chem.*, **2016**,**55**: 11342-11347
- [6] Sun B, Liu X F, Li X Y, et al. *Angew. Chem. Int. Ed.*, **2020**, **59**:203-208
- [7] Guan S, Souquet-Basiege M, Toulemonde O, et al. *Chem. Mater.*, **2019**,**31**:9819-9830
- [8] Nakamitsu M, Imai H, Oaki Y, et al. *ACS Sensors*, **2020**,**5**: 133-139
- [9] Soreno Z V, Puguan J M C, Kim H, et al. *Mater. Chem. Phys.*, **2020**,**240**:122297
- [10] Turchetti D A, Santana A J, Duarte L G T A, et al. *Polymer*, **2019**,**177**:65-72
- [11] Zhang W, Ji X, Peng B J, et al. *Adv. Funct. Mater.*, **2020**, **30**:1906463
- [12] Zhang W, Ji X, Chen K, et al. *Prog. Org. Coat.*, **2019**,**137**: 105280
- [13] Liao W M, Li X N, Zeng Q, et al. *J. Mater. Chem. C*, **2019**, **7**:15136-15140
- [14] Shakirova O, Protsenko A, Protsenko A, et al. *Inorg. Chim. Acta*, **2020**,**500**:119246
- [15] Ajeeb Y H, Minchenya A A, Klimovich P G, et al. *J. Appl. Spectrosc.*, **2019**,**86**:788-794
- [16] Wang P, Chen Z R, Li H H, et al. *Chinese J. Struct. Chem.*, **2019**,**38**:1485-1493
- [17] Hao P, Wang W, Shen J, et al. *Dalton Trans.*, **2020**,**49**:1847-1853
- [18] Liu G N, Xu R D, Zhao R Y, et al. *ACS Sustainable Chem. Eng.*, **2019**,**7**:18863-18873
- [19] Taylor W V, Cammack C X, Shubert S A, et al. *Inorg. Chem.*, **2019**,**58**:16330-16345
- [20] Zhang Y, Tso C Y, Inigo J S, et al. *Appl. Energy*, **2019**,**254**: 113690
- [21] Tom L, Kurup M R P. *Dalton Trans.*, **2019**,**48**:16604-16614
- [22] Jonane I, Anspoks A, Aquilanti G, et al. *Acta Mater.*, **2019**, **179**:26-35
- [23] Mande H M, Ghalsasi P S, Navamoney A. *Polyhedron*, **2015**, **91**:141-149
- [24] Troyano J, Zapata E, Perles J, et al. *Inorg. Chem.*, **2019**,**58**: 3290-3301
- [25] Yang K, Li S L, Zhang F Q, et al. *Inorg. Chem.*, **2016**,**55**: 7323-7325
- [26] Bloomquist D R, Willett R D. *Coord. Chem. Rev.*, **1982**,**47**: 125-164
- [27] Bloomquist Darrell R, Pressprich Mark R, Willett Roger D, et al. *J. Am. Chem. Soc.*, **1988**,**110**:7391-7398
- [28] Fu Z X, Lin J, Wang L, et al. *Cryst. Growth Des.*, **2016**,**16**: 2322-2327
- [29] Gupta S, Pandey T, Singh A K. *Inorg. Chem.*, **2016**,**55**:6817-6824
- [30] Huitorel B, El Moll H, Utrera-Melero R, et al. *Inorg. Chem.*, **2018**,**57**:4328-4339
- [31] Taylor W V, Cammack C X, Shubert S A, et al. *Inorg. Chem.*, **2019**,**58**:16330-16345
- [32] Landee C P, Roberts S A, Willett R D. *J. Chem. Phys.*, **1978**,**68**:4574-4577
- [33] Vishwakarma A K, Kumari R, Ghalsasi P S, et al. *J. Mol. Struct.*, **2017**,**1141**:93-98
- [34] Liu J C, Liao W Q, Li P F, et al. *Angew. Chem. Int. Ed.*, **2020**,**59**:3495-3499
- [35] Liu X X, Zhu Q, Chen D, et al. *Angew. Chem. Int. Ed.*, **2020**,**59**:2745-2749
- [36] Anderson J E, Cai J Q, Davies A G. *J. Chem. Soc., Perkin Trans. 2*, **1997**,**2**:2633-2637
- [37] Sheldrick G M. *Acta Crystallogr. Sect. C-Struct. Chem.*, **2015**, **71**:3-8
- [38] Bloomquist D R, Willett R D. *J. Am. Chem. Soc.*, **1981**,**103**: 2615-2619
- [39] Mande H M, Ghalsasi P S, Navamoney A. *Polyhedron*, **2015**, **91**:141-149